

## ARTICLE OPEN



# In vivo correlation of serotonin transporter and 1B receptor availability in the human brain: a PET study

Jonas E. Svensson <sup>1,2,✉</sup>, Mikael Tiger <sup>1</sup>, Pontus Plavén-Sigra<sup>1,2</sup>, Christer Halldin<sup>1</sup>, Martin Schain<sup>2,3</sup> and Johan Lundberg <sup>1</sup>

© The Author(s) 2022

Synaptic serotonin levels in the brain are regulated by active transport into the bouton by the serotonin transporter, and by autoreceptors, such as the inhibitory serotonin (5-HT) 1B receptor which, when activated, decreases serotonin release. Animal studies have shown a regulatory link between the two proteins. Evidence of such coupling could translate to an untapped therapeutic potential in augmenting the effect of selective serotonin reuptake inhibitors through pharmacological modulation of 5-HT<sub>1B</sub> receptors. Here we will for the first time in vivo examine the relationship between 5-HT<sub>1B</sub> receptors and serotonin transporters in the living human brain. Seventeen healthy individuals were examined with PET twice, using the radioligands [<sup>11</sup>C]AZ10419369 and [<sup>11</sup>C]MADAM for quantification of the 5-HT<sub>1B</sub> receptor and the 5-HT transporter, respectively. The binding potential was calculated for a set of brain regions, and the correlations between the binding estimates of the two radioligands were studied. [<sup>11</sup>C]AZ10419369 and [<sup>11</sup>C]MADAM binding was positively correlated in all examined brain regions. In most cortical regions the correlation was strong, e.g., frontal cortex,  $r(15) = 0.64$ ,  $p = 0.01$  and parietal cortex,  $r(15) = 0.8$ ,  $p = 0.0002$  while in most subcortical regions, negligible correlations was observed. Though the correlation estimates in cortex should be interpreted with caution due to poor signal to noise ratio of [<sup>11</sup>C]MADAM binding in these regions, it suggests a link between two key proteins involved in the regulation of synaptic serotonin levels. Our results indicate a need for further studies to address the functional importance of 5-HT<sub>1B</sub> receptors in treatment with drugs that inhibit serotonin reuptake.

*Neuropsychopharmacology* (2022) 47:1863–1868; <https://doi.org/10.1038/s41386-022-01369-3>

## INTRODUCTION

Major depressive disorder (MDD) is ranked by WHO as the third leading cause of years lost to disability, followed by migraine (position six) and anxiety disorders (position eight). Together they account for 13% of years lost to disability globally [1]. The pathophysiology of these brain disorders is largely unknown but they do share a commonality in that the serotonin (5-HT) system is implicated in all three [2–4]. The first choice of pharmacological treatment for MDD and most anxiety disorders are selective serotonin reuptake inhibitors (SSRIs) [5, 6], blocking the 5-HT transporter (5-HTT) [7]. The same class of drugs can be effective when treating migraine [8], alongside triptanes. In contrast to SSRIs, triptanes act as agonists at the 5-HT 1B receptor (5-HT<sub>1B</sub>) and are recommended as acute treatment for migraine headaches [9]. Modulation of the 5-HT<sub>1B</sub> receptor has also been suggested to be efficacious in psychiatric conditions [10, 11]. In Sweden around 10% of all citizens filled a prescription of an SSRI 2019 [12]. There is a large unmet need in improving the efficacy and speed of therapeutic onset of SSRIs. Augmentation with 5-HT<sub>1B</sub> modulating drugs could be effective in this regard [13]. To effectively design such treatments schemes the in vivo relationship between the two proteins should be better mapped out.

The serotonin transporter and the two G-protein coupled, inhibitory, 5-HT receptors 1A and 1B are central to the regulation

of serotonergic activity in the brain [14]. 5-HTT is exclusively located pre-synaptically and reduces synaptic 5-HT levels through transport back into serotonergic neurons [14]. 5-HT 1A and B receptors act both as heteroreceptors in projection areas, and as autoreceptors. 5-HT<sub>1A</sub> autoreceptors are predominantly located in the raphe nuclei, while 1B receptors are located presynaptically also in projection areas. Upon binding to a 5-HT<sub>1B</sub> autoreceptor, 5-HT inhibits formation of cAMP and downstream cellular responses, thus decreasing release of 5-HT to the synapse [11]. Interestingly, a direct link between 5-HT<sub>1B</sub> autoreceptors and 5-HTT have been suggested, with increased serotonin reuptake upon 5-HT<sub>1B</sub> receptor activation in synaptosomes, as well as decreased 5-HTT activity after 5-HT<sub>1B</sub> receptor antagonist administration [15, 16]. Vice versa, exposure to SSRIs have been shown to decrease 5-HT<sub>1B</sub> receptor mRNA and 5-HT<sub>1B</sub> receptor availability in the raphe nuclei in rats and non-human primates [10, 17], and increase 5-HT<sub>1B</sub> receptor availability in cortical areas in humans [18]. While 5-HT<sub>1A</sub> receptor modulation have been extensively explored with regards to psychiatric disorders in general and, more specifically, has been suggested to augment the effect of SSRI treatment in depression [19], relatively little focus has been directed towards the 5-HT<sub>1B</sub> receptor in this respect. Given that both 5-HTT and 5-HT<sub>1B</sub> are key proteins in the regulation of 5-HT signal transduction, there could well exist an untapped potential

<sup>1</sup>Centre for Psychiatry Research, Department of Clinical Neuroscience, Karolinska Institutet & Stockholm Health Care Services, Region Stockholm, Karolinska University Hospital, SE-171 76 Stockholm, Sweden. <sup>2</sup>Neurobiology Research Unit, Copenhagen University Hospital, Copenhagen, Denmark. <sup>3</sup>Antaros Medical AB, Bioventure Hub, Mölndal, Sweden. ✉email: [jonas.svensson@ki.se](mailto:jonas.svensson@ki.se)

in concomitant SSRI treatment and pharmacological modulation of 5-HT<sub>1B</sub> receptors.

Positron emission tomography (PET) studies have shown a high correlation between brain regions for the in vivo concentration of most examined proteins related to the serotonin system [20]. This means that if an individual has a high concentration (relative to other individuals) of 5-HT<sub>1B</sub> in e.g., occipital cortex the same individual is likely to have a high concentration of 5-HT<sub>1B</sub> also in other brain regions. However less is known of the covariance between proteins, e.g., if an individual has high levels of 5-HTT in one brain region, does this predict high levels of 5-HT<sub>1B</sub> in the same region? Knowledge of the interplay between the proteins regulating 5-HT neurotransmission could generate novel treatment strategies. To this end, several published PET studies have explored the correlation between 5-HTT and 5-HT<sub>1A</sub> receptors in healthy subjects indicating brain region specific correlations, with some variability between studies [21, 22]. To our knowledge there exists no study reporting on the correlation between 5-HTT and 5-HT<sub>1B</sub> receptors in vivo. With the development of selective 5-HT<sub>1B</sub> radioligands such as [<sup>11</sup>C]AZ10419369 [23], 5-HT<sub>1B</sub> receptor binding can now be examined in relation to 5-HTT in vivo.

In this study we examined 17 healthy controls with PET and two radioligands during the same day: [<sup>11</sup>C]MADAM and [<sup>11</sup>C]AZ10419369, to quantify the density of 5-HTT and 5-HT<sub>1B</sub> respectively. This aim of the study was to examine correlations between the two proteins in relevant brain regions.

## MATERIALS AND METHODS

### Subjects

Seventeen volunteers (13 females; 4 males) were recruited. Recruitment was done by advertisement in local newspapers, followed by a physical visit where subjects were screened by a psychiatrist or a resident physician supervised by a psychiatrist, with: (1) the Mini- International Neuropsychiatric Interview (M.I.N.I.) [24]; (2) a physical examination, including a neurological examination; (3) blood tests (complete blood count, aspartate amino transferase, alanine amino transferase, gamma-glutamyl transferase, sodium, potassium, creatinine, calcium, albumin, thyroid stimulating hormone, glucose) and urine tests (drug screen; pregnancy test when indicated); and (4) MRI of the brain. All subjects had no history of disease involving the central nervous system, including current or previous psychiatric disorders, and were aged 23–75 years ( $47 \pm 14$ , mean  $\pm$  SD). The study was approved by the Research Ethics Committee in Stockholm, Sweden, and the Radiation Safety Committee at Karolinska University Hospital, Stockholm. All subjects gave verbal and written informed consent before participation. Part of the data have previously served as healthy control data for a longitudinal 5-HTT PET study on depression [25].

### Radiochemistry

Subjects were examined with PET and [<sup>11</sup>C]MADAM (for quantification of 5-HTT) and [<sup>11</sup>C]AZ10419369 (for quantification of 5-HT<sub>1B</sub> receptors) on the same day and in a random order. For details on radioligand preparation see [26] for [<sup>11</sup>C]MADAM and [23] for [<sup>11</sup>C]AZ10419369. The injected radioactivity for [<sup>11</sup>C]MADAM was  $408 \pm 85$  MBq, the specific radioactivity was  $231 \pm 134$  GBq/ $\mu$ mol, and injected mass was  $0.93 \pm 1.28$   $\mu$ g. For [<sup>11</sup>C]AZ10419369 the injected radioactivity was  $382 \pm 63$  MBq, the specific radioactivity was  $330 \pm 183$  GBq/ $\mu$ mol, and injected mass was  $0.82 \pm 0.78$   $\mu$ g.

### MRI and PET experimental procedure

T1-weighted MRI images were acquired using a 3T GE Signa system (GE Medical Systems, USA). A high-resolution research tomograph (Siemens Molecular Imaging, USA) with a maximum spatial resolution of  $\sim 2$  mm full-width-half-maximum [27] was used for all PET examinations. Transmission scans were performed prior to each PET measurement to correct for signal attenuation.

In each PET-experiment a saline solution containing [<sup>11</sup>C]MADAM was injected into an antecubital vein as a bolus (<10 s). The cannula was then flushed with 10 mL saline. For both radioligands emission data were acquired continuously for 93 minutes, and subsequently binned into

consecutive time frames. For [<sup>11</sup>C]MADAM 38 frames with the following definitions: nine 10 s, two 15 s, three 20 s, four 30 s, four 1 min, four 3 min and twelve 6 min frames and for [<sup>11</sup>C]AZ10419369 37 frames: eight 10 s, five 20 s, four 30 s, four 1 min, four 3 min and twelve 6 min frames.

### Regions of interest

FreeSurfer (version 6.0, <http://surfer.nmr.mgh.harvard.edu/>) [28] was used to delineate brain regions on the T1-weighted MRIs of all subjects. We chose to quantify the binding in brain regions where both radioligands have a moderate to high binding: amygdala, anterior cingulate gyrus (ACC), posterior cingulate gyrus (PCC), caudate, hippocampus, insular cortex, putamen, and thalamus, but also in cortical regions of interest for both neurological and psychiatric diseases where the [<sup>11</sup>C]MADAM binding is comparatively low: occipital, parietal, frontal and temporal cortex (see Supplementart Fig. S1 for a visualization of the included brain regions). Both radioligands have high binding in pallidum, however this region was not included since equilibrium is not reached during the time of the PET-experiment for either radioligand [29].

Delineation of raphe was performed using an automatic process, described previously [25], where information from FreeSurfer brainstem [30] and the time-weighted summated [<sup>11</sup>C]MADAM image is used to generate a median raphe mask containing 65 voxels and a dorsal raphe mask of 116 voxels (see Supplementary Fig. S2 for a visualization of the raphe masks).

### Image preprocessing and quantification

Dynamic PET images were corrected for head motion using a between-frame-correction algorithm implemented in SPM12 (Wellcome Department of Cognitive Neurology, University College, London, UK). Frames were realigned to the first six-minute frame (21–27 min of the scan for both radioligands). For each individual, the T1-weighted MR-image was co-registered to time-weighted summated PET-images yielding one co-registration matrix per radioligand. The co-registration matrix was then used to project regions of interest (ROIs) on the realigned dynamic PET-image to derive regional time-activity curves.

From the time-activity curves binding potential ( $BP_{ND}$ ) was calculated for each ROI using the non-invasive Logan plot fitted with multilinear regression [31]. For [<sup>11</sup>C]AZ10419369,  $t^*$  was set to 33 min, corresponding to 10 frames. For [<sup>11</sup>C]MADAM, a  $t^*$  of 45 min (corresponding to 8 frames) was used in order to account for the high density of 5-HTT in the raphe nuclei [32]. The reference region efflux rate constant ( $k_2'$ ) was derived using the simplified reference tissue model [33]; for [<sup>11</sup>C]MADAM the  $k_2'$  value from putamen was used [34] and for [<sup>11</sup>C]AZ10419369 average  $k_2'$  in frontal- and occipital cortex, caudatus, insula and putamen was used. Cerebellar gray matter was defined as described previously [35] and used as reference region for both radioligands [29, 36].

To extract  $BP_{ND}$  for the raphe nuclei masks, parametric images were generated using the 3D stationary wavelet aided parametric imaging procedure, where the non-invasive Logan plot, fitted with multilinear regression, is applied on time activity curves from individual voxels [37]. This method has been shown to effectively reduce noise in small brain regions [38]. For each individual, the dorsal and median raphe masks were applied both to the [<sup>11</sup>C]MADAM and [<sup>11</sup>C]AZ10419369 parametric-images to obtain the corresponding binding estimates in these small brainstem regions.

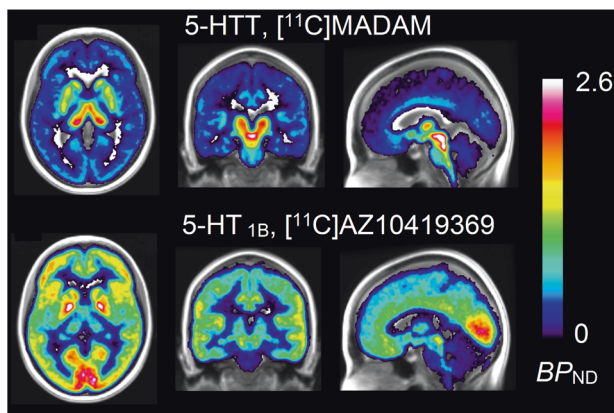
For visualizations, the parametric images were registered to MNI-space [39] and averaged across individuals for both radioligands.

### Statistics

We had no a priori hypothesis of the direction of a putative correlation, or in which brain regions an association would be most likely. Based on this, we performed an exploratory analysis of the data. Thus, we did not apply the conventional null hypothesis significance testing, where an alpha is set for error control, but rather we applied a fisherian interpretation of the calculated  $p$  values [40], where a low  $p$ -value is interpreted as indirect inductive evidence against the null hypothesis (here defined as no association between the radioligands); the smaller the  $p$ -value, the more unlikely is the occurrence of these data in the event that the null hypothesis is true (i.e., the more probable explanation is that the null-hypothesis is false and should be rejected). Since no claims regarding type I error rate was made, no correction for multiple comparisons was performed. It is possible also under a strict fisherian interpretation to set a threshold for "significance". However, since this terminology is intimately

**Table 1.** Regional [ $^{11}\text{C}$ ]MADAM and [ $^{11}\text{C}$ ]AZ10419369  $BP_{\text{ND}}$  and correlation.

Region	[ $^{11}\text{C}$ ]MADAM $BP_{\text{ND}}$ (mean $\pm$ SD)	[ $^{11}\text{C}$ ]AZ10419369 $BP_{\text{ND}}$ (mean $\pm$ SD)	correlation	$p$ value
Temporal cortex	0.26 $\pm$ 0.04	0.86 $\pm$ 0.10	0.60	0.01
Frontal cortex	0.22 $\pm$ 0.04	1.05 $\pm$ 0.17	0.64	0.01
Parietal cortex	0.23 $\pm$ 0.04	0.95 $\pm$ 0.14	0.80	0.0002
Posterior cingulate	0.39 $\pm$ 0.07	0.91 $\pm$ 0.16	0.44	0.09
Occipital cortex	0.27 $\pm$ 0.05	1.21 $\pm$ 0.15	0.37	0.16
Anterior cingulate	0.40 $\pm$ 0.06	1.04 $\pm$ 0.19	0.23	0.40
Amygdala	0.93 $\pm$ 0.12	0.93 $\pm$ 0.2	0.13	0.62
Caudate Nucleus	0.73 $\pm$ 0.12	0.93 $\pm$ 0.13	0.29	0.28
Hippocampus	0.38 $\pm$ 0.08	0.45 $\pm$ 0.12	0.51	0.04
Insula	0.54 $\pm$ 0.07	1.05 $\pm$ 0.18	0.42	0.11
Putamen	1.12 $\pm$ 0.15	1.27 $\pm$ 0.18	0.11	0.68
Thalamus	1.17 $\pm$ 0.10	0.53 $\pm$ 0.09	0.38	0.15
Accumbens	1.04 $\pm$ 0.13	1.79 $\pm$ 0.3	0.01	0.96
Median raphe	2.88 $\pm$ 0.47	0.97 $\pm$ 0.33	0.19	0.48
Dorsal raphe	3.15 $\pm$ 0.42	1.41 $\pm$ 0.31	0.40	0.12

**Fig. 1** Mean parametric images of [ $^{11}\text{C}$ ]MADAM and [ $^{11}\text{C}$ ]AZ10419369 examinations overlaid on an averaged MR-image. Images are aligned in the same plane.  $BP_{\text{ND}}$ , non-displaceable binding potential.

connected to type 1 error control under null hypothesis significance testing framework, and might lead to confusion, we did not apply any  $p$  value threshold, nor did we use the term “significance” here. To describe the strength of the association between variables, we used the following heuristic: a correlation estimate between 0–0.19 was described as negligible, 0.2–0.39 as weak, 0.40–0.59 as moderate, 0.6–0.79 as strong and 0.8–1 as very strong [41].

Both 5-HTT and 5-HT<sub>1B</sub> have been shown to decrease with age [18, 42], a positive correlation between the two radioligands can therefore be expected even with no true underlying association between the examined proteins, or a true association might be masked by noise added by an age effect. Partial Pearson correlation coefficients were therefore calculated, corrected for age, using the R-package “ppcor” [43].

## RESULTS

Average  $BP_{\text{ND}}$  in the examined brain regions is reported for both [ $^{11}\text{C}$ ]MADAM and [ $^{11}\text{C}$ ]AZ10419369 in Table 1 and visualized in Fig. 1.

[ $^{11}\text{C}$ ]AZ10419369 and [ $^{11}\text{C}$ ]MADAM binding was positively correlated within all 15 examined brain regions. In many cortical regions the correlation point estimate was strong, e.g., temporal cortex,  $r(15) = 0.6$ ,  $p = 0.01$  and parietal cortex,  $r(15) = 0.8$ ,

$p = 0.0002$ . In most subcortical regions the correlation estimate was negligible, e.g., putamen,  $r(15) = 0.11$ ,  $p = 0.68$  and amygdala,  $r(15) = 0.13$ ,  $p = 0.62$ , with hippocampus as the exception,  $r(15) = 0.51$ ,  $p = 0.04$  (Table 1, Fig. 2).

## DISCUSSION

In this PET study, we report on the in vivo association between 5-HTT and 5-HT<sub>1B</sub> receptor binding in the human brain. We observe a strong positive correlation between the binding estimates in cortical regions and hippocampus, and negligible to weak correlations in subcortical regions, such as the striatum.

In some, but not all, cortical regions 5-HT<sub>1B</sub> receptor binding correlated with 5-HTT binding. While 5-HTT is only expressed on 5-HT neurons and with a low density in cortex [44], autoradiography studies show a high density of the 5-HT<sub>1B</sub> receptor in the cerebral cortex [44] where it is expressed both as autoreceptors, and as heteroreceptors on non-serotonergic neurons, including GABAergic and cholinergic neurons [11]. It is not possible to differentiate between auto- and heteroreceptors from PET data, and in rodent neocortex there are studies in support of both 5-HT<sub>1B</sub> auto- and heteroreceptor availability [11, 45, 46]. Thus, the correlations between cortical 5-HTT and 5-HT<sub>1B</sub> receptors may entail either the autoreceptor or the heteroreceptor population in cortex, or both. In the hippocampus we observed a correlation of 0.51 between the two examined proteins. Hippocampus is a subcortical brain region with demonstrated 5-HT<sub>1B</sub> autoreceptor function [11, 47]. It has been suggested that the delay in onset of SSRI antidepressant effect is related to downstream modulation of inhibitory serotonin autoreceptors [48]. This idea is supported by observations of a twofold increase in extracellular serotonin concentration in hippocampus following SSRI exposure in 5-HT<sub>1B</sub> receptor knockout mice [47], and increased 5-HT<sub>1B</sub> receptor binding after a single oral dose of SSRI in healthy controls [49]. In line with this reasoning, increased 5-HT<sub>1B</sub> receptor binding in the hippocampus has been demonstrated with PET after rapid acting MDD treatments such as ketamine [50] and electroconvulsive therapy [51]. In previous PET studies of 5-HT<sub>1B</sub> receptor binding in unmedicated patients with depression low 5-HT<sub>1B</sub> receptor binding in hippocampus has been reported [52, 53]. It could be hypothesized that 5-HTT inhibition leads to upregulation of 5-HT<sub>1B</sub> receptors in projection regions, as has been found in healthy volunteers [49]. Though the relationship between 5-HTT and 5-HT<sub>1B</sub> receptors in man in vivo needs to be explored further, such

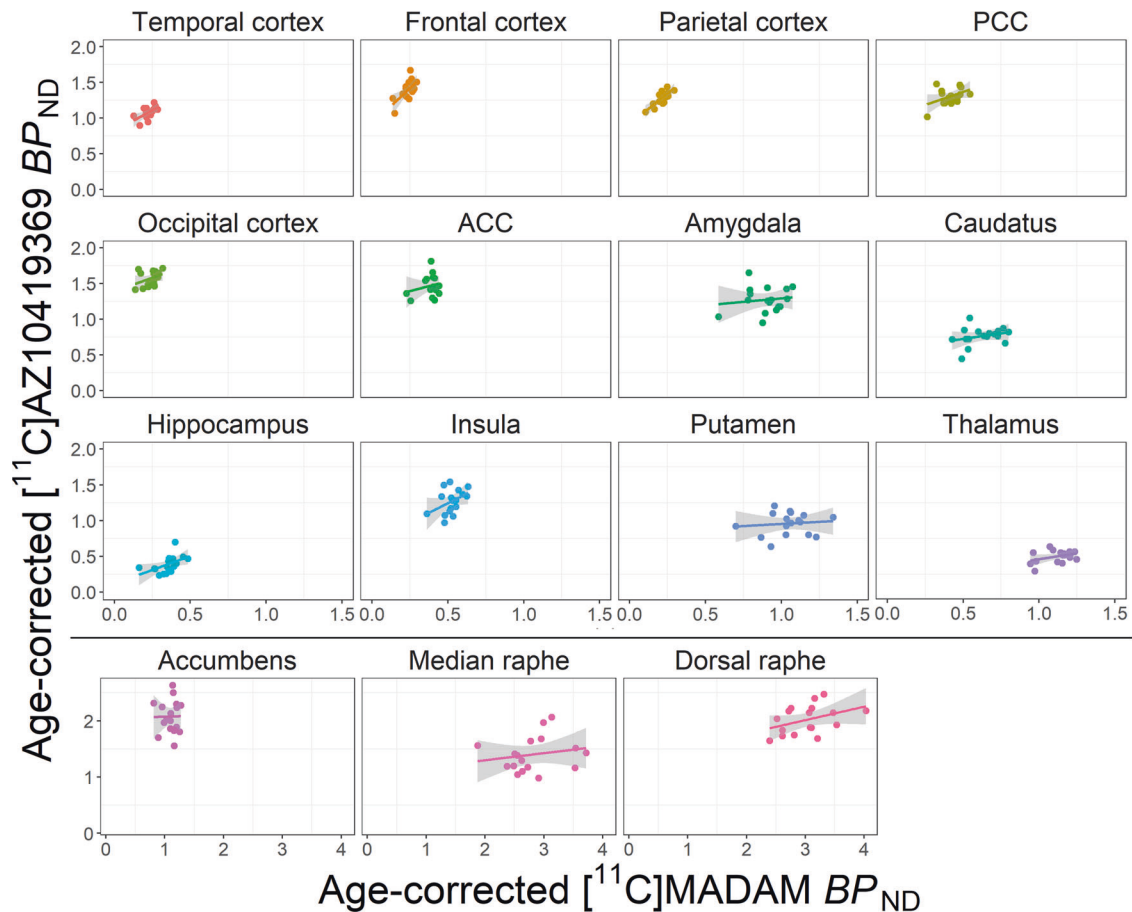


**Fig. 2** Scatter plots of  $[^{11}\text{C}]\text{AZ10419369}$  and  $[^{11}\text{C}]\text{MADAM}$  binding in different brain regions. Plotted  $\text{BP}_{\text{ND}}$  values are corrected for age. For purposes of visualization separate scales have been used in the three lowest panels (Accumbens, median and dorsal raphe nuclei, situated below the black horizontal line). Regression lines with 95% confidence interval in shaded gray. See Supplementary Fig. S3 for a version of the figure with individual scales for each region. ACC Anterior cingulate cortex, PCC Posterior cingulate cortex,  $\text{BP}_{\text{ND}}$ , non-displaceable binding potential.

dynamics could be leveraged in designing novel treatments schemes.

The discrepancy between the strong correlations observed in cortical regions and the negligible to weak correlations in some subcortical regions could possibly be explained by a lack of autoreceptors in the subcortical regions. Studies reporting on lesioning of serotonergic neurons has shown either increased or not affected 5-HT<sub>1B</sub> receptor binding in nucleus caudatus and putamen [45, 54, 55], indicating that 5-HT<sub>1B</sub> receptors in these regions are not autoreceptors. In humans, nucleus caudatus and putamen stands out as the only regions with non-detectable age related decrease in 5-HT<sub>1B</sub> receptor binding [18]. Thus, we observed correlations in brain regions with documented 5-HT<sub>1B</sub> autoreceptor expression, but not in regions where the 5-HT<sub>1B</sub> receptor predominantly is expressed as a heteroreceptor. For the subcortical region thalamus, 5-HT<sub>1B</sub> receptor localization is relatively unexplored. However, the discrepancy between high thalamic 5-HTT binding and low 5-HT<sub>1B</sub> receptor binding in this region is well in line with previous reports [44]. Thus, while the 5-HT<sub>1B</sub> receptor is inhibitory, with decreased serotonin release upon autoreceptor activation, regional differences in 5-HT<sub>1B</sub> receptor localization may lead to different modulation of neurotransmission in different regions, such as when signaling is stimulated through 5-HT<sub>1B</sub> receptor inhibition of inhibitory GABA interneurons, as can be seen with 5-HT<sub>1B</sub> receptor induced increase of dopamine release [56, 57]. Moreover, regionally different changes of 5-HT<sub>1B</sub> receptor binding have been

demonstrated after 5-HTT inhibition, with increased 5-HT<sub>1B</sub> receptor binding in cortical regions and reduced 5-HT<sub>1B</sub> receptor binding in raphe nuclei [49].

An important caveat to the discussion above is that  $[^{11}\text{C}]\text{MADAM}$  show very low binding in most cortical regions, with  $\text{BP}_{\text{ND}}$ s in our data ranging between 0.22 (frontal cortex) and 0.54 (insula). Thus, the signal-to-background is relatively poor, which in theory should make it more difficult to detect a correlation induced by specific binding to the target proteins. Despite this, we observe the strongest correlations in regions with the lowest  $[^{11}\text{C}]\text{MADAM}$   $\text{BP}_{\text{ND}}$  (Table 1). One possible explanation could be a correlation in the radioactive uptake between the two radioligands in the reference region. Such correlation could be caused by similarities in non-specific binding, differing cerebellar anatomy between subjects, or small discrepancies in ROI delineation. If, for instance, an individual has an anatomical variant with wider cerebellar sulci, increasing radioactive spill out to cerebrospinal fluid, this will dilute the uptake for the reference region in both PET experiments. A correlation of radioligand uptake in the reference tissue, regardless of whether it is methodologically induced, or if it originates from similarities in non-specific binding, will have a larger impact on  $\text{BP}_{\text{ND}}$  correlation estimates in brain regions with low densities of the target proteins. Supporting this explanation is the observation of a strong correlation between the two radioligands in centrum semiovale, a region purportedly only containing white matter ( $r = 0.66$ ,  $p = 0.01$ , controlled for age). An analysis of

interindividual variability of radioactive uptake in the non-displaceable compartment would require an arterial input function and is not possible within the present dataset. Such an analysis should be considered as part of the further explorations of the 5-HTT and 5-HT<sub>1B</sub> receptors *in vivo*.

The age range of the study participants was relatively wide (23–75 years). The binding estimates for both radioligands is known to be inversely correlated with age [18, 42]. In the statistical analysis we have attempted to correct for this using age as a covariate. The age effect may in part be caused by spill-out of radioactivity due to age related decrease in gray matter volume. In order to further explore this, we performed an analysis correcting for the volume of each brain region instead of age. In this analysis the correlation estimates were attenuated in cortical regions and strengthened in thalamus (Supplementary Table S1).

Twelve of the seventeen subjects performed both the [<sup>11</sup>C]MADAM and [<sup>11</sup>C]AZ10419369 examinations during the same day. For five subjects, logistical difficulties made same day experiments impossible. Three subjects therefore performed the examinations with one day apart and two subjects with seven days apart. An analysis restricted to the 12 subjects with same day experiments showed similar correlation estimates compared with the full sample in most examined brain regions (Supplementary Table S2).

In conclusion, we found moderate to strong correlations between 5-HTT and 5-HT<sub>1B</sub> receptors in brain regions with documented distributions of 5-HT<sub>1B</sub> autoreceptors. Such associations are in line with previously described functional relationship between two key regulators of the serotonin system. However, the fact that the strongest correlations were found in regions with the lowest signal-to-background ratio raises the caveat that associations might be, in part, induced by factors not related to specific binding of the radioligands. The clinical potential of the interplay between 5-HTT and 5-HT<sub>1B</sub> receptors should be investigated in patients treated with SSRI.

## REFERENCES

- World Health Organization. Global Health Estimates 2016: Disease burden by Cause, Age, Sex, by Country and by Region, 2000–2016. Geneva; 2018.
- Lapin IP, Oxenkrug GF. Intensification of the central serotonergic processes as a possible determinant of the thymoleptic effect. *Lancet*. 1969;293:132–6.
- Ressler KJ, Nemeroff CB. Role of serotonergic and noradrenergic systems in the pathophysiology of depression and anxiety disorders. *Depress Anxiety*. 2000;12:2–19.
- Hamel E, Currents H. Serotonin and migraine: biology and clinical implications. *Cephalalgia*. 2007;27:1293–1300.
- The National Institute for Health and Care Excellence (NICE). Generalised anxiety disorder and panic disorder in adults: management. 2011.
- Warden D, Rush A, Trivedi M, Fava M, Wisniewski S. The STAR\*D project results: a comprehensive review of findings. *Curr Psychiatry Rep*. 2008;9:449–59.
- Lundberg J, Tiger M, Landén M, Halldin C, Farde L. Serotonin transporter occupancy with TCAs and SSRIs: a PET study in patients with major depressive disorder. *Int J Neuropsychopharmacol*. 2012;15:1167–72.
- Burch R. Antidepressants for preventive treatment of migraine. *Curr Treat Options Neurol*. 2019;21:18.
- The National Institute for Health and Care Excellence (NICE). Headaches in over 12s: diagnosis and management. 2012.
- Yang K-C, Stepanov V, Amini N, Martinsson S, Takano A, Bundgaard C, et al. Effect of clinically relevant doses of vortioxetine and citalopram on serotonergic PET markers in the nonhuman primate brain. *Neuropsychopharmacology*. 2019;44:1706–13.
- Tiger M, Varnäs K, Okubo Y, Lundberg J. The 5-HT(1B) receptor - a potential target for antidepressant treatment. *Psychopharmacol (Berl)*. 2018;235:1317–34.
- The Swedish National Board of Health and Welfare. Statistics on Pharmaceuticals 2019. 2020:2020-4-6708. <https://www.socialstyrelsen.se/statistik-och-data/statistik/statistikdatabasen/>.
- Ruf MB, Bhagwagar Z. The 5-HT<sub>1B</sub> receptor: a novel target for the pathophysiology of depression. *Curr Drug Targets*. 2009;10:1118–38.
- Charnay Y, Léger L. Brain serotonergic circuitries. *Dialogues Clin Neurosci*. 2010;12:471–87.
- Hagan CE, McDevitt RA, Liu Y, Furay AR, Neumaier JF. 5-HT(1B) autoreceptor regulation of serotonin transporter activity in synaptosomes. *Synapse*. 2012;66:1024–34.
- Montañez S, Munn JL, Owens WA, Horton RE, Daws LC. 5-HT<sub>1B</sub> receptor modulation of the serotonin transporter *in vivo*: Studies using KO mice. *Neurochem Int*. 2014;73:127–31.
- Anthony JP, Sexton TJ, Neumaier JF. Antidepressant-induced regulation of 5-HT<sub>1B</sub> mRNA in rat dorsal raphe nucleus reverses rapidly after drug discontinuation. *J Neurosci Res*. 2000;61:82–87.
- Nord M, Cselényi Z, Forsberg A, Rosenqvist G, Tiger M, Lundberg J, et al. Distinct regional age effects on [<sup>11</sup>C]AZ10419369 binding to 5-HT<sub>1B</sub> receptors in the human brain. *Neuroimage*. 2014;103:303–8.
- Whale R, Terao T, Cowen P, Freemantle N, Geddes J. Pindolol augmentation of serotonin reuptake inhibitors for the treatment of depressive disorder: a systematic review. *J Psychopharmacol*. 2008;24:513–20.
- Beliveau V, Ozenne B, Strother S, Greve DN, Svarer C, Knudsen GM, et al. The structure of the serotonin system: A PET imaging study. *Neuroimage*. 2020;205:116240.
- Lundberg J, Borg J, Halldin C, Farde LA. PET study on regional coexpression of 5-HT<sub>1A</sub> receptors and 5-HTT in the human brain. *Psychopharmacol (Berl)*. 2007;195:425–33.
- Strupp-Levitsky M, Miller JM, Rubin-Falcone H, Zanderigo F, Milak MS, Sullivan G, et al. Lack of association between the serotonin transporter and serotonin 1A receptor: an *in vivo* PET imaging study in healthy adults. *Psychiatry Res Neuroimaging*. 2016;255:81–86.
- Pierson ME, Andersson J, Nyberg S, McCarthy DJ, Finnema SJ, Varnäs K, et al. [<sup>11</sup>C]AZ10419369: A selective 5-HT<sub>1B</sub> receptor radioligand suitable for positron emission tomography (PET). Characterization in the primate brain. *Neuroimage*. 2008;41:1075–85.
- Sheehan DV, Lecrubier Y, Sheehan KH, Amorim P, Janavs J, Weiller E, et al. The Mini-International Neuropsychiatric Interview (M.I.N.I.): The development and validation of a structured diagnostic psychiatric interview for DSM-IV and ICD-10. *J Clin Psychiatry*. 1998;59:22–33.
- Svensson JE, Svanborg C, Plavén-Sigraý P, Kaldo V, Halldin C, Schain M, et al. Serotonin transporter availability increases in patients recovering from a depressive episode. *Transl Psychiatry*. 2021;11:264.
- Halldin C, Lundberg J, Sóvágó J, Gulyás B, Guilloteau D, Vercouillie J, et al. [<sup>11</sup>C]MADAM, a new serotonin transporter radioligand characterized in the monkey brain by PET. *Synapse*. 2005;58:173–83.
- Varrone A, Sjöholm N, Eriksson L, Gulyás B, Halldin C, Farde L. Advancement in PET quantification using 3D-OP-OSEM point spread function reconstruction with the HRRT. *Eur J Nucl Med Mol Imaging*. 2009;36:1639–50.
- Fischl B. FreeSurfer. *Neuroimage*. 2012;62:774–81.
- Varnäs K, Nyberg S, Halldin C, Varrone A, Takano A, Karlsson P, et al. Quantitative analysis of [<sup>11</sup>C]AZ10419369 binding to 5-HT<sub>1B</sub> receptors in human brain. *J Cereb Blood Flow Metab*. 2010;31:113–23.
- Iglesias JE, Van Leemput K, Bhatt P, Casillas C, Dutt S, Schuff N, et al. Bayesian segmentation of brainstem structures in MRI. *Neuroimage*. 2015;113:184–95.
- Matheson GJ, Stenkrona P, Cselényi Z, Plavén-Sigraý P, Halldin C, Farde L, et al. Reliability of volumetric and surface-based normalisation and smoothing techniques for PET analysis of the cortex: A test-retest analysis using [<sup>11</sup>C]SCH-23390. *Neuroimage*. 2017;155:344–53.
- Schain M, Tóth M, Cselényi Z, Arakawa R, Halldin C, Farde L, et al. Improved mapping and quantification of serotonin transporter availability in the human brainstem with the HRRT. *Eur J Nucl Med Mol Imaging*. 2013;40:228–37.
- Lammertsma AA, Hume SP. Simplified reference tissue model for PET receptor studies. *Neuroimage*. 1996;4:153–8.
- Nørgaard M, Ganz M, Svarer C, Frokjaer VG, Greve DN, Strother SC, et al. Optimization of preprocessing strategies in Positron Emission Tomography (PET) neuroimaging: A [<sup>11</sup>C]DASB PET study. *Neuroimage*. 2019;199:466–79.
- Svensson JE, Schain M, Plavén-Sigraý P, Cervenka S, Tiger M, Nord M, et al. Validity and reliability of extraatrial [<sup>11</sup>C]raclopride binding quantification in the living human brain. *Neuroimage*. 2019;202:116143.
- Lundberg J, Odano I, Olsson H, Halldin C, Farde L. Quantification of [<sup>11</sup>C]MADAM binding to the serotonin transporter in the human brain. *J Nucl Med*. 2005;46:1505–15.
- Cselényi Z, Olsson H, Farde L, Gulyás B. Wavelet-Aided Parametric Mapping of Cerebral Dopamine D<sub>2</sub> Receptors Using the High Affinity PET Radioligand FLB 457. *Neuroimage*. 2002;17:47–60.
- Schain M, Tóth M, Cselényi Z, Arakawa R, Halldin C, Farde L, et al. Improved mapping and quantification of serotonin transporter availability in the human brainstem with the HRRT. *Eur J Nucl Med Mol Imaging*. 2013;40:228–37. <https://doi.org/10.1007/s00259-012-2260-3>.
- Evans AC, Collins DL, Mills SR, Brown ED, Kelly RL, Peters TM 3D statistical neuroanatomical models from 305 MRI volumes. 1993 IEEE Conf. Rec. Nucl. Sci. Symp. Med. Imaging Conf., 1993. p. 1813–7 vol. 3.

40. Perezgonzalez JD, Fisher, Neyman-Pearson or NHST? A tutorial for teaching data testing. *Front Psychol.* 2015;6:223.
41. Swinscow TDV *Statistics at Square One.* Ninth EditBMJ Publishing Group 1997; 1997.
42. Karrer TM, McLaughlin CL, Guaglianone CP, Samanez-Larkin GR. Reduced serotonin receptors and transporters in normal aging adults: a meta-analysis of PET and SPECT imaging studies. *Neurobiol Aging.* 2019;80:1–10.
43. Kim S. ppcor: An R package for a fast calculation to semi-partial correlation coefficients. *Commun Stat Methods.* 2015;22:665–74.
44. Varnäs K, Halldin C, Hall H. Autoradiographic distribution of serotonin transporters and receptor subtypes in human brain. *Hum Brain Mapp.* 2004;22:246–60.
45. Pranzatelli MR, Durkin MM, Farmer M. Plastic responses of neonatal 5-hydroxytryptamine1B receptors to 5,7-dihydroxytryptamine lesions mapped by quantitative autoradiography. *Int J Dev Neurosci.* 1996;14:621–9.
46. Nautiyal KM, Tanaka KF, Barr MM, Tritschler L, Le Dantec Y, David DJ, et al. Distinct circuits underlie the effects of 5-HT1B receptors on aggression and impulsivity. *Neuron.* 2015;86:813–26.
47. Nautiyal KM, Tritschler L, Ahmari SE, David DJ, Gardier AM, Hen R. A lack of serotonin 1B autoreceptors results in decreased anxiety and depression-related behaviors. *Neuropsychopharmacology.* 2016;41:2941–50.
48. Nutt DJ. The neuropharmacology of serotonin and noradrenaline in depression. *Int Clin Psychopharmacol.* 2002;17 Suppl 1:S1–12.
49. Nord M, Finnema SJ, Halldin C, Farde L. Effect of a single dose of escitalopram on serotonin concentration in the non-human and human primate brain. *Int J Neuropsychopharmacol.* 2013;16:1577–86.
50. Tiger M, Veldman ER, Ekman C-J, Halldin C, Svenningsson P, Lundberg J. A randomized placebo-controlled PET study of ketamine's effect on serotonin1B receptor binding in patients with SSRI-resistant depression. *Transl Psychiatry.* 2020;10:159.
51. Tiger M, Gärde M, Tateno A, Matheson GJ, Sakayori T, Nogami T, et al. A positron emission tomography study of the serotonin1B receptor effect of electroconvulsive therapy for severe major depressive episodes. *J Affect Disord.* 2021;294:645–51.
52. Murrrough JW, Czermak C, Henry S, Nabulsi N, Gallezot J-D, Gueorguieva R, et al. The effect of early trauma exposure on serotonin type 1B receptor expression revealed by reduced selective radioligand binding. *Arch Gen Psychiatry.* 2011;68:892–900.
53. Tiger M, Farde L, Rück C, Varrone A, Forsberg A, Lindefors N, et al. Low serotonin1B receptor binding potential in the anterior cingulate cortex in drug-free patients with recurrent major depressive disorder. *Psychiatry Res Neuroimaging.* 2016;253:36–42.
54. Offord SJ, Ordway GA, Frazer A. Application of [125I]iodocyanopindolol to measure 5-hydroxytryptamine1B receptors in the brain of the rat. *J Pharm Exp Ther.* 1988;244:144 LP–153.
55. Verge D, Daval G, Marcinkiewicz M, Patey A, el Mestikawy S, Gozlan H, et al. Quantitative autoradiography of multiple 5-HT1 receptor subtypes in the brain of control or 5,7-dihydroxytryptamine-treated rats. *J Neurosci.* 1986;6:3474 LP–3482.
56. Dell LE, Parsons LH. Serotonin1B receptors in the ventral tegmental area modulate cocaine-induced increases in nucleus accumbens dopamine levels. *J Pharm Exp Ther.* 2004;311:711 LP–719.
57. Yan Q-S, Zheng S-Z, Yan S-E. Involvement of 5-HT1B receptors within the ventral tegmental area in regulation of mesolimbic dopaminergic neuronal activity via GABA mechanisms: a study with dual-probe microdialysis. *Brain Res.* 2004;1021:82–91.

## AUTHOR CONTRIBUTIONS

JS performed the PET-experiments, the data analysis and manuscript preparation; MT, PPS and MS contributed to the data analysis and manuscript preparation; CH contributed to data acquisition; JL was responsible for study design, data analysis and manuscript writing. All authors reviewed and approved the final version of this manuscript.

## FUNDING

This work was funded by the Swedish Research Council (2013-09304), StratNeuro, and a donation from Birgitta and Sten Westerberg. Johan Lundberg was supported by Region Stockholm (higher clinical research appointment); Jonas Svensson was supported by grants from the Swedish Mental Health Fund and the Swedish Society of Medicine; Pontus Plavén-Sigraý was supported by the Swedish Society of Medicine. All authors declare no competing financial interests in relation to the work described. Open access funding provided by Karolinska Institute.

## COMPETING INTERESTS

The authors declare no competing interests.

## ADDITIONAL INFORMATION

**Supplementary information** The online version contains supplementary material available at <https://doi.org/10.1038/s41386-022-01369-3>.

**Correspondence** and requests for materials should be addressed to Jonas E. Svensson.

**Reprints and permission information** is available at <http://www.nature.com/reprints>

**Publisher's note** Springer Nature remains neutral with regard to jurisdictional claims in published maps and institutional affiliations.



**Open Access** This article is licensed under a Creative Commons Attribution 4.0 International License, which permits use, sharing, adaptation, distribution and reproduction in any medium or format, as long as you give appropriate credit to the original author(s) and the source, provide a link to the Creative Commons licence, and indicate if changes were made. The images or other third party material in this article are included in the article's Creative Commons licence, unless indicated otherwise in a credit line to the material. If material is not included in the article's Creative Commons licence and your intended use is not permitted by statutory regulation or exceeds the permitted use, you will need to obtain permission directly from the copyright holder. To view a copy of this licence, visit <http://creativecommons.org/licenses/by/4.0/>.

© The Author(s) 2022